Chemical Physics Letters 691 (2018) 14–21

Contents lists available at ScienceDirect

Chemical Physics Letters

journal homepage: www.elsevier.com/locate/cplett

Research paper

Study of structural, optical properties and electronic structure of PTCDI-C5 organic nanostructure

Mustafa Kurban [a,*], Bayram Gündüz [b]

[a] Department of Electronics and Automation, Ahi Evran University, 40100 Kırşehir, Turkey
[b] Department of Science Education, Faculty of Education, Muş Alparslan University, 49250 Muş, Turkey

ARTICLE INFO

Article history:
Received 26 September 2017
In final form 25 October 2017
Available online 1 November 2017

Keywords:
Organic nanostructures
Optical properties
Electrical conductivity
Electronic structure
Density-functional theory
Refractive index

ABSTRACT

This work reports the change in the structural, electronic, spectroscopic and optical properties of N,N′-Dipentyl-3,4,9,10-perylenedicarboximide (PTCDI-C5) small molecule via experimental and theoretical techniques. Experimental and simple models were taken into consideration to calculate the refractive index (n) of PTCDI-C5 from its energy gap (E_g) data. Electrical conductance was recorded. UV, FT-IR and FT-Raman spectra characteristics and the electronic properties of PTCDI-C5 were also recorded time-dependent (TD) DFT approach based on optimized structure with different solvent environments. The results herein obtained reveal that PTCDI-C5 material is suitable for UV and chemical sensors due to its good optoelectronic paramaters.

1. Introduction

In recent years, organic semiconductors have received enormous attention for many electronic, optoelectronic, and photonic applications [1] such as solar cells [2–5] photovoltaics [4,5] light emitting diodes [4,6] sensors [7,8], chemical sensors [9], vapour sensors [10], gas sensors [11,12] and photodetectors [13]. The semiconductors have also been investigated by performing density functional theory (DFT) [14–16]. Among the semiconductors, the perylenediimides (PTCDIs) which are n-type materials are the most widely used in areas including electronic and optoelectronic applications [17] because of their high thermal and photo-stability properties under visible light beam [18–25]. PTCDIs also have a propensity to self-assemble into one-dimensional nanostructures through π-π stacking. [17,26-28]. In addition, fluorescent conjugated polymers including PTCDIs are used as sensory materials for the detection of ultra-trace analytes [29]. In the literature, a series of available perylene and its derivatives (PTCDI-M, where M = C_5, C_8, C_{10}, BP_2C_{10}, OSC, etc.) were studied in various electronic, photovoltaic and optoelectronic devices. For instance, the sensory properties of PTCDI-C_{10}, PTCDI-Br_2C_{10} and PTCDI-BP_2C_{10} molecules have been investigated and found that the response values of these perylene derivatives as gas sensors increased with increasing concentration and decreasing nanostructure size [30]. Cholesterol-derived PTCDIs used as gas sensing materials have a high sensitivity amine sensor properties [31]. Moreover, logic functionality in the form of a basic complementary inverter was demonstrated by combining n-channel (PTCDI) and p-channel (HTP) nanowire transistors [32].

As far as we are aware, there have been no any reports about the structural, electronic, spectroscopic and optical properties of N,N′-Dipentyl-3,4,9,10-perylenedicarboximide (PTCDI-C5) small molecule using quantum chemical calculations.

The sensing and optical properties of the related material were investigated in detail for different concentrations and solvents [33,34]. However, one of the most important parameter, which is recractive index (n), in optical parameters was not investigated for various relations. In here, we investigated the fundamental n from experimental measurement and various theoretical relations. In addition, the structural, electronic and spectroscopic properties of PTCDI-C5 molecule have been investigated by performing DFT calculations. The theoretically predicted the ultraviolet–visible (UV), Fourier Transform Infrared (FT-IR) and Fourier Transform Raman (FT-Raman) spectra characteristics, the highest occupied molecular orbital (HOMO), the lowest unoccupied molecular orbital (LUMO) and the frontier molecular orbital energy gap (HOMO–LUMO difference in energy gap, E_g) of PTCDI-C5 small molecule have been investigated using time dependent (TD)-DFT based on optimized structure with different solvent environments. The results including E_g and UV spectra have been compared with the experimentally measured values and have been discussed in detail.

* Corresponding author.
E-mail address: mkurbanphys@gmail.com (M. Kurban).

https://doi.org/10.1016/j.cplett.2017.10.053
0009-2614/

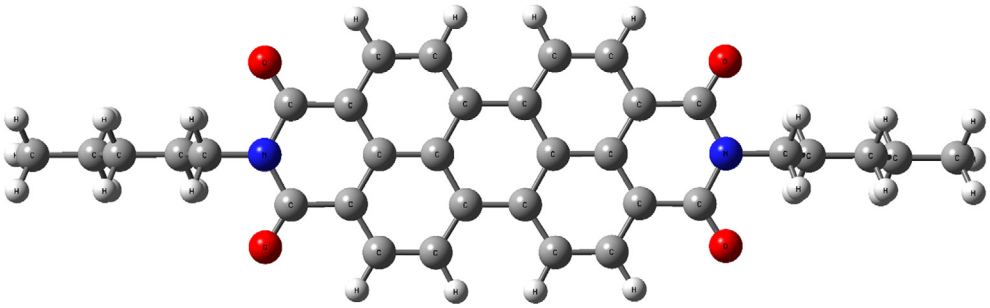

Fig. 1. Optimized ground state geometry of PTCDI-C5 molecule with atom numbering calculated by B3LYP/6-311-G(d, p).

2. Experimental details

Experimental details such as preparation processes of the solutions and UV measurements of the N,N′-Dipentyl-3,4,9,10-perylene dicarboximide (PTCDI-C5) material for different solvents and molarities are given in detail in Refs. [34,35].

3. Computational details

The structural, electronic and spectroscopic properties of PTCDI-C5 have been investigated using DFT [35] at the B3LYP level. The exchange term of B3LYP consists of hybrid Hartree–Fock (HF) and local spin density (LSD) exchange functions with Becke's gradient correlation to LSD Exchange [36]. The correlation term of B3LYP consists of the Vosko, Wilk, and Nusair (VWN3) local correlation functional [37] and Lee, Yang, and Parr (LYP) correlation functional [38]. This functional also gives its accurate frequencies that play an important role in thermochemistry. The 6-311G(d, p) basis set has been used in the calculations. The calculations have been performed using the GAUSSIAN09 program package [39]. Various spin multiplicities were investigated and it has been found that PTCDI-C5 have spin singlet as the most stable (minimum total energy). The geometry of PTCDI-C5 were optimised without imposing any symmetrical constraints and the lowest total energy configuration was assumed as the global minimum case. The structure is taken as the local minima on potential energy surface having positive vibration frequencies. After geometric optimization, TD-DFT method used to get maximum wavelengths and compared with the experimental UV absorption and E_g of PTCDI-C5 small molecule.

4. Results and discussion

4.1. Structural analysis

Optimized ground state structure and process of geometry optimization of PTCDI-C5 with atom numbering calculated by B3LYP/6-311-G(d, p) is shown in Figs. 1 and 2, respectively. From TD-DFT calculations, the positive vibrational spectra, that is no any kind of imaginary frequency, are found that the optimized geometry of the PTCDI-C5 compound is located at stationary point on the potential energy surface. The geometrical optimization results reveal that the structure with minimum total energy of PTCDI-C5 small molecule is the C_1 form. All the 205 fundamental modes of vibrations of PTCDI-C5 were found to be IR and Raman active suggesting that the molecule possesses a non-centro symmetric structure. This realization leads us to the conclusion that PTCDI-C5 small molecule should recommend for non-linear optical applications such as telecommunications, opto-electronics, medicine, etc. For visual comparison the simulated FT-IR and FT-Raman spectra of PTCDI-C5 are shown in Figs. 3 and 4, respectively.

4.2. Ultraviolet–visible spectroscopy

The molar extinction coefficient (ε), which is also known as the molar absorptivity and molar attenuation coefficient is an intrinsic property of the species. The ε can be given depends on the Beer-Lamber law [40],

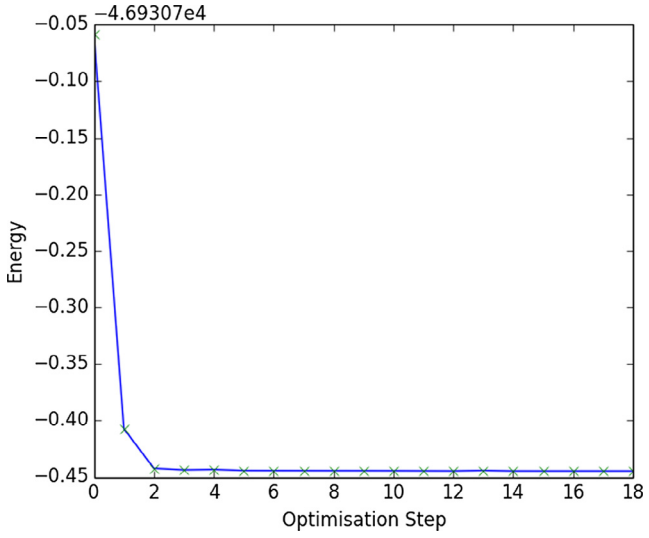

Fig. 2. Process of geometry optimization of PTCDI-C5 depending on energy.

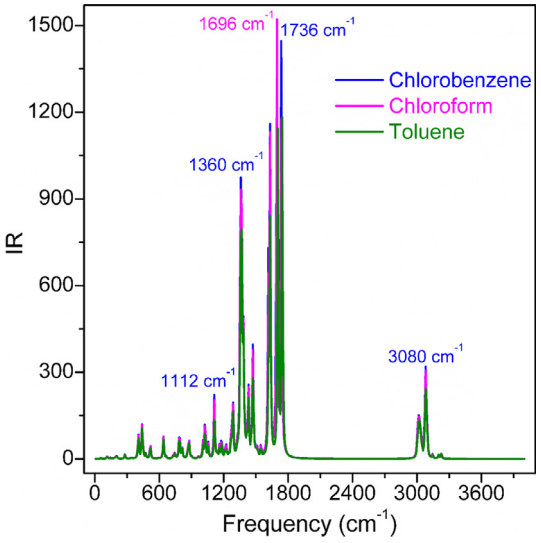

Fig. 3. FT-IR spectra of PTCDI-C5.

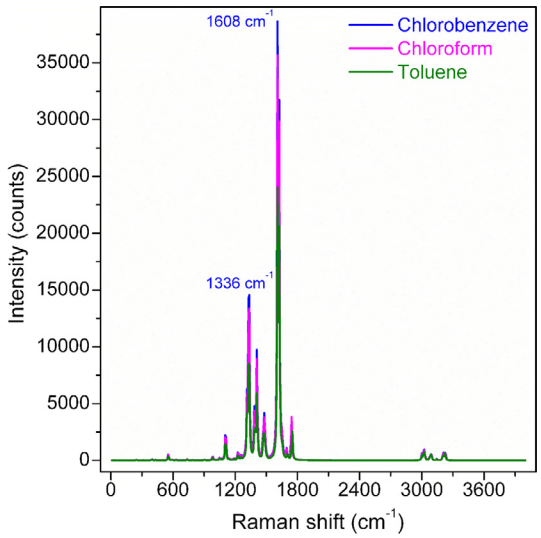

Fig. 4. FT-Raman spectra of PTCDI-C5.

$$\varepsilon = \frac{Abs}{CL} \tag{1}$$

where Abs is the absorbance, C is the concentration of a solution sample and L is the path length of the sample. The molar absorptivity values of the PTCDI-C5 organic material for chlorobenzene, chloroform and toluene solvents were experimentally obtained from Eq. (1). Fig. 5(a–c) indicates the molar absorptivity plots vs. wavelength (λ) of the PTCDI-C5 organic material for chlorobenzene, chloroform and toluene solvents, respectively. The right side of the figures shows theoretical molar absorptivity values, while the left side of the figures shows experimental molar absorptivity values. The wavelengths of the peaks of experimental and theoretical molar extinction coefficient (molar absorptivity) were observed at various wavelength values as seen in Fig. 5(a–c).

As seen in Fig. 5(a–c), for chlorobenzene, chloroform and toluene solvents, the experimental molar extinction coefficient exhibits maximum values at 528, 524 and 526 nm, while the theoretical molar absorptivity exhibits maximum values at 543, 532.15 and 532.15 nm, respectively. Also, the experimental molar extinction coefficients for chlorobenzene, chloroform and toluene solvents exhibit three dominant peaks in visible (V) region, while the theoretical molar absorptivity (or molar extinction coefficient) exhibits one peak in the same region and for the same solvents. However, near ultraviolet (NUV) region, the theoretical peaks of the molar absorptivity for chlorobenzene, chloroform and toluene solvents are higher than the experimental peaks of the molar absorptivity and are observed at lower wavelength (332.87, 331.49 and 331.95 nm) for the same solvents, respectively. Obtained results suggest that the experimental molar extinction coefficient values are compatible with theoretical ones and theoretical UV spectra can be eliminated some low vibration according to experimental UV spectra. Such an outcome can be related either to the selected exchange–correlation functional, to the application of the harmonic vibrational approximation, or to specific effects (e.g. aggregation) not accounted for in the calculation. Moreover, chlorobenzene, chloroform and toluene solvents have an effect on molar extinction coefficients.

4.3. Refractive index values for different solvents, concentrations and relations

To obtain the refractive index values of the PTCDI-C5 solved in chlorobenzene, chloroform and toluene solvents, n_{gd} many equations such as Reddy, Ravindra, Kumar-Singh, Herve-Vandamme and Moss [41,42] were used together with the reported the direct (E_{gd}) and indirect (E_{gid}) optical band gap values of the PTCDI-C5 [33] as seen in Table 1(a and b). The direct n_{gd} and indirect n_{gid} values of the PTCDI-C5 for chlorobenzene, chloroform and toluene solvents were calculated by using related equations and were given in Table 1(a and b), respectively. Fig. 6(a and b) indicates n_{gd} and n_{gid} curves vs. solvents for various relations. As seen in Table 1a and in Fig. 6(a), the values for chloroform are the lowest, while the n_{gd} values for toluene are the highest. Similarly, the n_{gd} values obtained from Moss relation are the lowest, while the n_{gd} values obtained from Reddy relation are the highest. As seen in Table 1(a and b) and in Fig. 6(a and b), the n_{gd} and n_{gid} values for chloroform are the lowest, while the n_{gd} and n_{gid} values for toluene are the highest. Similarly, the n_{gd} and n_{gid} values obtained from Moss relation are the lowest, while the n_{gd} and n_{gid} values obtained from Reddy relation are the highest. Obtained results suggest that the direct n_{gd} values are lower than the indirect n_{gid} values.

To obtain the refractive index values of the PTCDI-C5 for different concentrations (0.654, 1.472, 4.410 and 6.618 mM) with Reddy, Ravindra, Kumar-Singh, Herve-Vandamme and Moss [41,42] relations, we used the direct and indirect optical band gap values from our previous work [31]. The n_{gd} and n_{gid} values of the PTCDI-C5 organic material for 0.654, 1.472, 4.410 and 6.618 mM were obtained by using related equations [41,42] and were given in Table 2(a and b), respectively. Fig. 7(a and b) indicates n_{gd} and n_{gid} curves vs. concentrations (molarities) for various relations. As seen in Table 2(a) and in Fig. 7 (a), the n_{gd} values for 6.618 mM are the highest, while the n_{gd} values for 0.654 mM are the lowest. On the other hand, the n_{gd} values obtained from Reddy relation are the highest, while the n_{gd} values obtained from Moss relation are the lowest. Obtained results suggest that the n_{gd} and n_{gid} values increase with increasing concentration.

4.4. Electrical conductance values for different solvents and concentrations

For electronic and optoelectronic devices, electrical conductance (σ_{elect}) plays a key role on performance of device. The σ_{elect} values of the PTCDI-C5 were obtained from the following equations [42,43],

$$\sigma_{elect} = \frac{\lambda nc}{2\pi} \tag{2}$$

where c is the velocity of light and n is the refractive index. We obtained the σ_{elect} values of the PTCDI-C5 for chlorobenzene, chloroform and toluene solvents. Fig. 8(a) shows the σ_{elec} curves vs. photon energy (E). As seen in Fig. 8(a), the electrical conductance exhibits the maximum values and peaks between about 2.3 and 2.85 eV. The electrical conductance values for toluene solvent are more different than that of the chlorobenzene and chloroform solvents.

The σ_{elec} values of the PTCDI-C5 for 0.654, 1.472, 4.410 and 6.618 mM were obtained from Eq. (2). Fig. 8(b) indicates the σ_{elect} curves vs. E. As seen in Fig. 8(b), the electrical conductance varies with concentrations and is order of around 10^3 S. Obtained results show that the electrical conductance can be controlled with concentrations. This may be an advantage for electronic and optoelectronic devices.

4.5. Amplitude properties of the PTCDI-C5 film

Amplitude image of the PTCDI-C5 film was recorded by a Park System, XE100 AFM (Gwanggyo-Ro, Korea). Fig. 9 shows the amplitude image ($10 \times 10\ \mu m^2$) of the PTCDI-C5 film. As seen in Fig. 9, PTCDI-C5 film shows nano and micro-rods. The amplitude of the PTCDI-C5 film was found to be 1.59 μm.

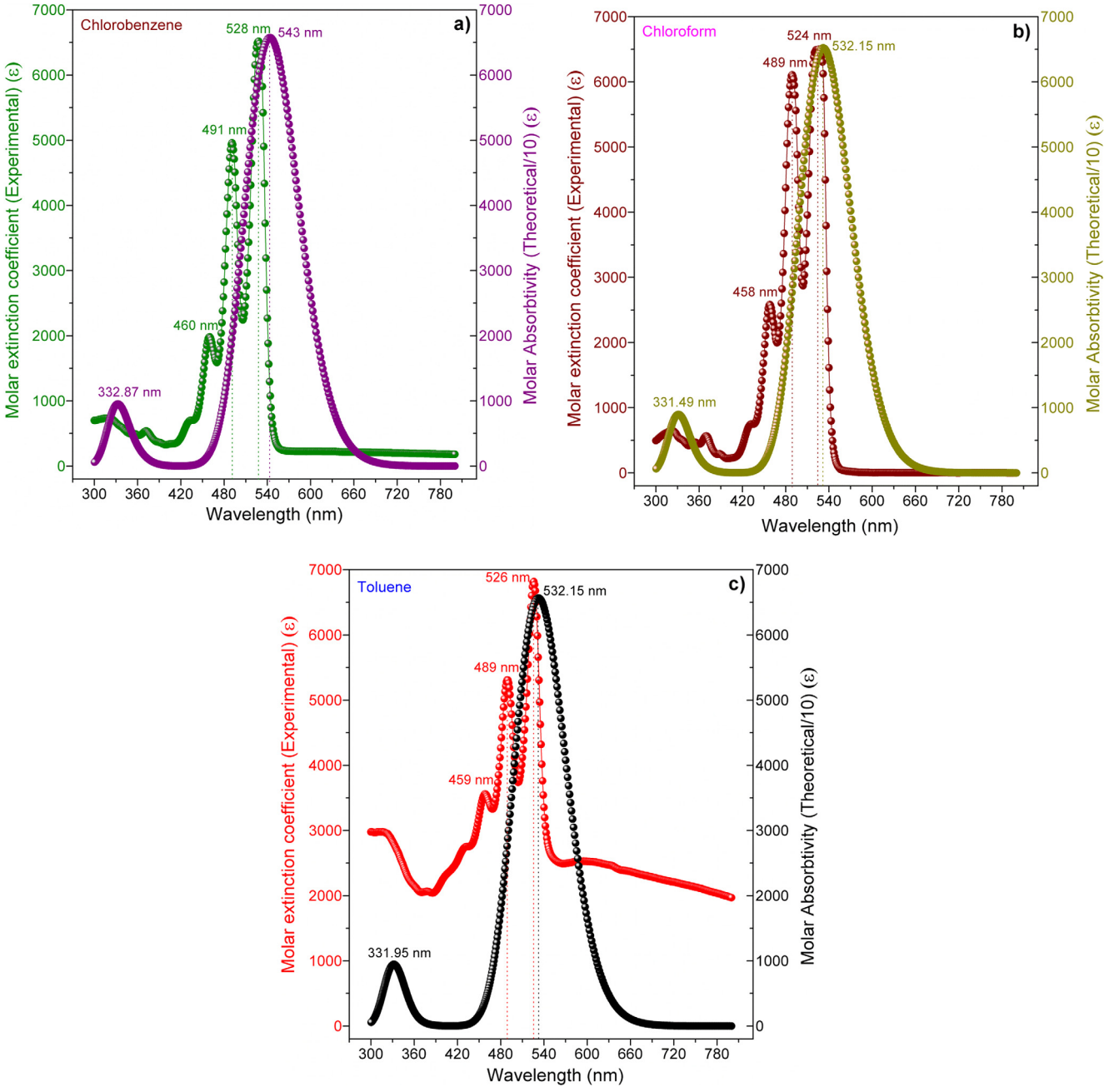

Fig. 5. The experimental and theoretical molar absorptivity plots vs. wavelength (λ) of the PTCDI-C5 organic material for a) chlorobenzene, b) chloroform and c) toluene solvents.

Table 1
The refractive index values of the PTCDI-C5 solutions for various relations and solvent obtained from (a) direct optical band gaps (E_{gd}) and (b) indirect optical band gaps (E_{gid}).

Solvents	n Values for direct optical band gaps				
	Moss	Ravindra	Herve-Vandamme	Reddy	Kumar-Singh
(a)					
Chloroform	2.542	2.672	2.569	2.996	2.582
Chlorobenzene	2.545	2.681	2.574	3.001	2.588
Toluene	2.565	2.724	2.601	3.029	2.614
(b)					
Chloroform	2.555	2.702	2.587	3.015	2.600
Chlorobenzene	2.562	2.718	2.597	3.025	2.610
Toluene	2.578	2.750	2.618	3.047	2.630

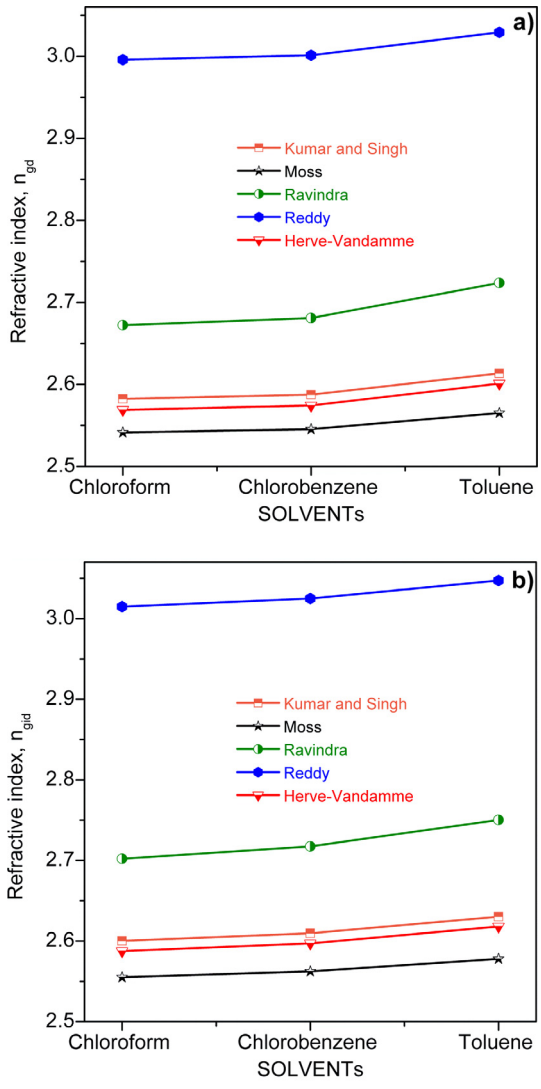

Fig. 6. The refractive index (n) curves vs. solvents of the PTCDI-C5 for various relations obtained from (a) direct optical band gaps (E_{gd}) and (b) indirect optical band gaps (E_{gid}).

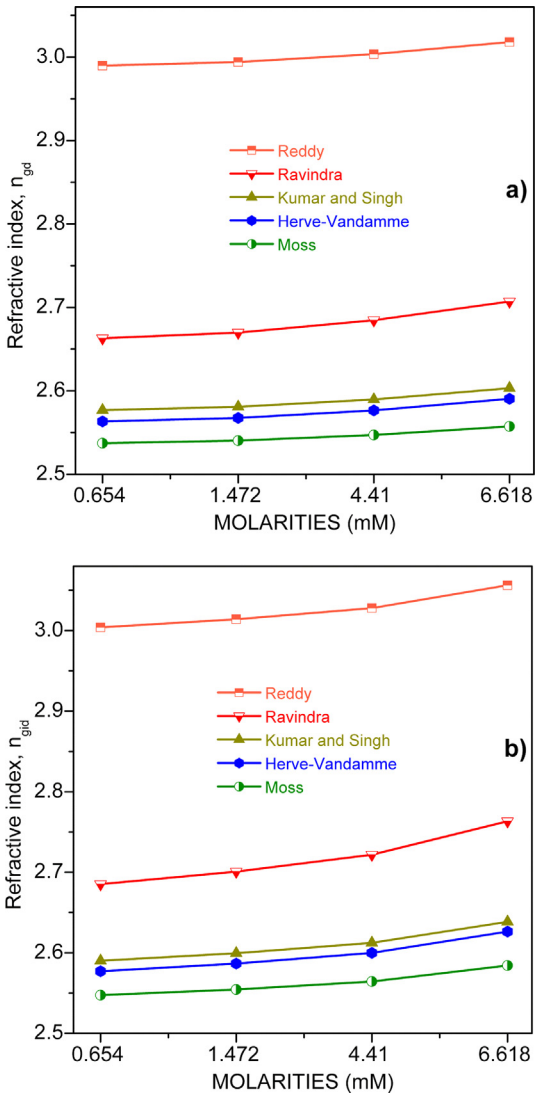

Fig. 7. The refractive index (n) curves vs. concentrations (molarities) of the PTCDI-C5 for various relations obtained from (a) direct optical band gaps (E_{gd}) and (b) indirect optical band gaps (E_{gid}).

4.6. Electronic band structure

The energy gap which is HOMO–LUMO difference in energy, is an significant parameter in measuring the electron conductivity. The experimental direct optical band gaps (E_{gd}), indirect optical band gaps (E_{gid}) depending on different solvents and concentrations (mM) and the energy gaps (E_g), obtained from DFT and TD-DFT calculations are tabulated in Table 3. The measured E_{gd} and E_{gid} for Chloroform solvent are about 2.277 and 2.229 eV, respectively, which is consistent with the theoretical E_g value (2.277 eV, HOMO = 5.956 eV and LUMO = 3.678 eV) obtained from DFT (see Table 3). From the results, one can conclude that toluene solvent with the lowering of the band gaps can be preferred for optoelectronic applications or devices, which prefer lower band gaps because the electronic transfer in the molecule PTCDI-C5 is easier. It implies that the HOMO-LUMO energy gap for toluene solvent compared to that of other solvent allows easy excitation of electrons from HOMO to LUMO. The energy gap values of compounds PTCDI, PTCDI-CN_2 and PTCDI-C_8 was also found to be 2.54 eV [44], 2.52 eV [45] and 2.20 eV [46], respectively.

In addition, the dispersion of the electronic bands for thicker PTCDI-C5 samples increases due to interacting layers and thus reduces the band gap energies as it seen in Table 3. We can also see that the band gap energies decrease with increment of the size of the materials at the nanoscale (see Table 3). This is the most remarkable feature of materials at nano level [47,48].

Table 2
The refractive index values of the PTCDI-C5 solutions for various relations and concentrations (mM) obtained from (a) direct optical band gaps (E_{gd}) and (b) indirect optical band gaps (E_{gid}).

Concentrations	n Values for direct optical band gaps				
	Moss	Ravindra	Herve-Vandamme	Reddy	Kumar-Singh
(a)					
0.654	2.537	2.663	2.563	2.990	2.577
1.472	2.540	2.670	2.568	2.994	2.581
4.41	2.547	2.685	2.57668	3.004	2.590
6.618	2.557	2.707	2.591	3.018	2.603
(b)					
0.654	2.547	2.685	2.577	3.004	2.590
1.472	2.555	2.701	2.587	3.014	2.600
4.41	2.564	2.722	2.600	3.028	2.612
6.618	2.584	2.763	2.626	3.056	2.639

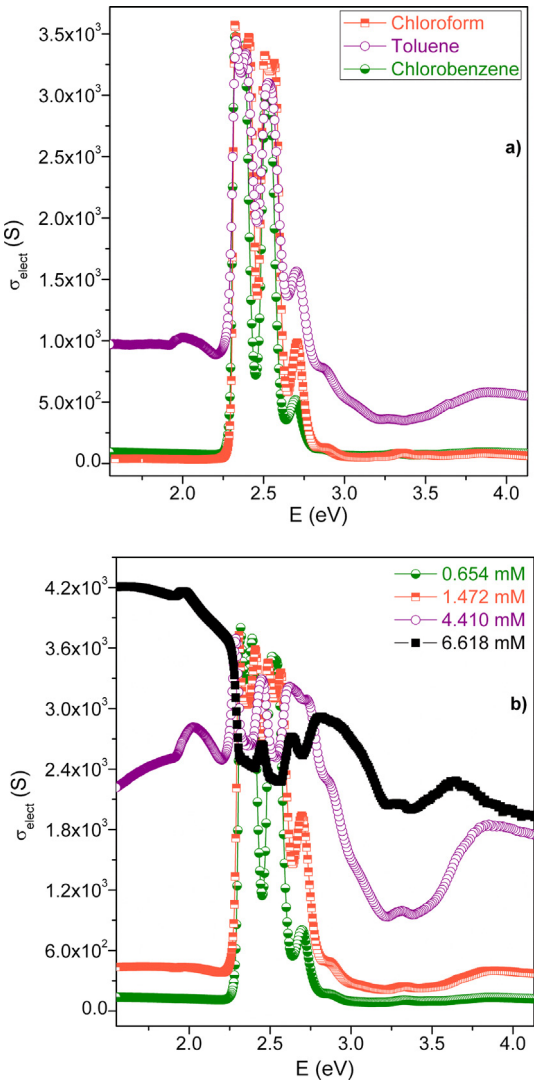

Fig. 8. The electrical conductance (σ_{elect}) curves vs. (E) of the PTCDI-C5 for different (a) solvents and (b) concentrations.

4.7. Theoretical analysis of Mulliken atomic charge and dipole moment

The Mulliken atomic charges (MAC) have a significant for quantum mechanical applications. MAC of PTCDI-C5 compound were gathered in Table 4. The charges of the atoms in the different positions show different charge with each other for some carbon atoms. For example, MAC of Carbon atom is mostly negative in PTCDI-C5 compound, however, the value of the average MAC of this atom is positive in PTCDI-C5 compound when carbon atom combined with O and N atoms. The C28 atom exhibits a positive charge the value of MAC is bigger than others. Hydrogen atom exhibits a positive charge because it is an acceptor atom.

The dipole moments are other important electronic properties. The bigger the dipole moment represents the stronger intermolecular interaction. The highest value of component of dipole moment along the z-axis (μ_z = −0.22 Debye) predicts large opposite charge separation in PTCDI-C5 compound. The corresponding total dipole moment has been calculated to be 0.23 Debye.

4.8. Analysis of density of state

The density of state (DOS) is important, because the occupied and unoccupied molecular orbitals can be seen on DOS spectrum.

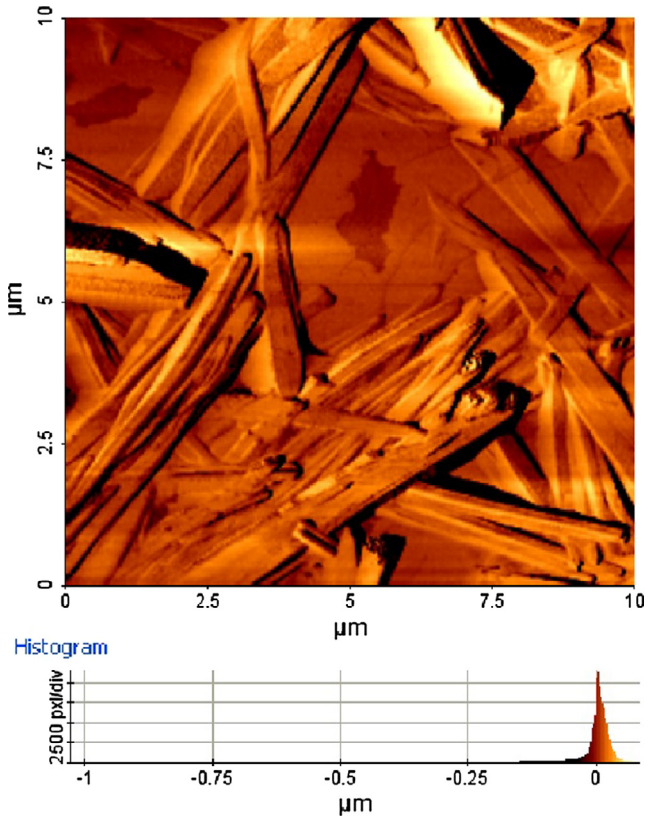

Fig. 9. The amplitude image (10 × 10 µm^2) of the PTCDI-C5 film.

DOS gives a representation of molecule orbitals (MOs) compositions and their contributions to chemical bonding. Using Mulliken population analysis, we have plotted DOS spectrum (see Fig. 10) for PTCDI-C5 using GaussSum 3.0 software [49]. From Fig. 10, the density of localized states has a sharply increasing tendency in the region of between −15 and -10 eV. The DOS analysis also indicates that the energy gap of PTCDI-C5 has the highest value (2.27 eV) in chloroform therefore it is less reactive compared with other solvents. PTCDI-C5 with Chlorobenzene is found to be the highest energy of HOMO value (−6.19 eV).

4.9. Radial distribution function and probability density

Fig. 11 shows the radial distribution functions (RDFs) analysis for carbon-carbon (C-C), carbon-hydrogen (C-H), carbon-nitrogen (C-N), oxygen-hydrogen (O-H) and carbon-oxygen (C-O), interactions of PTCDI-C5 small molecule. The RDFs is calculated for each atomic pairs of optimized PTCDI-C5 molecule. One can see that C-H has a narrower and higher distribution than the other pair interactions because of the weaker bond and the low atomic weight of the H atom. Moreover, there is a slight difference

Table 3
The experimental direct optical band gaps (E_{gd}, eV), indirect optical band gaps (E_{gid}, eV) depending on different solvents and concentrations (mM) and the energy gaps (E_g, eV), obtained from DFT and TD-DFT calculations.

Solvents	[a]E_{gd}	[a]E_{gid}	DFT	TD-DFT	Concentrations	[b]E_{gd}	[b]E_{gid}
Chloroform	2.277	2.229	2.277	2.511	**0.654**	2.292	2.256
Chlorobenzene	2.263	2.204	2.277	2.541	**1.472**	2.281	2.231
Toluene	2.194	2.151	2.280	2.545	**4.41**	2.257	2.197
					6.618	2.221	2.13

[a,b] Refs. [30,31].

Table 4
Mullkien atomic charges of PTCDI-C5.

Atoms	Mulliken atomic charges	Atoms	Mulliken atomic charges
O1	−0.362106	C36	−0.221075
O2	−0.362068	C37	−0.224693
O3	−0.362075	C38	−0.224720
O4	−0.362125	C39	−0.294702
N5	−0.501479	C40	−0.294671
N6	−0.501474	H41	0.105877
C7	−0.006018	H42	0.105890
C8	−0.006041	H43	0.105907
C9	−0.007139	H44	0.105897
C10	−0.007219	H45	0.111294
C11	−0.007258	H46	0.111277
C12	−0.007121	H47	0.111288
C13	0.092277	H48	0.111293
C14	0.092352	H49	0.138675
C15	−0.251411	H50	0.138628
C16	−0.251426	H51	0.138599
C17	−0.251431	H52	0.138674
C18	−0.251379	H53	0.115868
C19	−0.024501	H54	0.115948
C20	−0.024490	H55	0.115805
C21	−0.024458	H56	0.116026
C22	−0.024490	H57	0.109356
C23	−0.018321	H58	0.109345
C24	−0.018352	H59	0.109354
C25	−0.018340	H60	0.109324
C26	−0.018344	H61	0.107467
C27	0.530456	H62	0.107438
C28	0.530539	H63	0.107427
C29	0.530514	H64	0.107486
C30	0.530504	H65	0.107734
C31	−0.074925	H66	0.103720
C32	−0.074941	H67	0.103718
C33	−0.195667	H68	0.107733
C34	−0.195613	H69	0.103699
C35	−0.221046	H70	0.103726

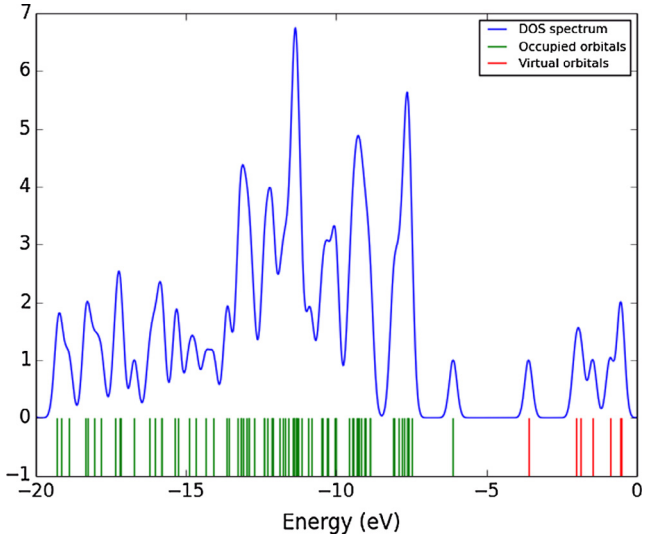

Fig. 10. Density of state (DOS) spectrum of PTCDI-C5 obtained Mulliken population analysis.

between C-C and C-O atoms. For C atoms, C-O is slightly shorter than C-C and C-N interactions; for H, C-C is shorter than C-H. For all of the combinations, C-H has stronger interactions than the other ones. To study the influence of interactions of the atoms in the molecule, we also performed the probability distribution depending on the coordination number (Fig. 12). The coordination number of C-N and C-O interactions significantly decrease; for C-C and C-H interactions we have observed some fluctuations.

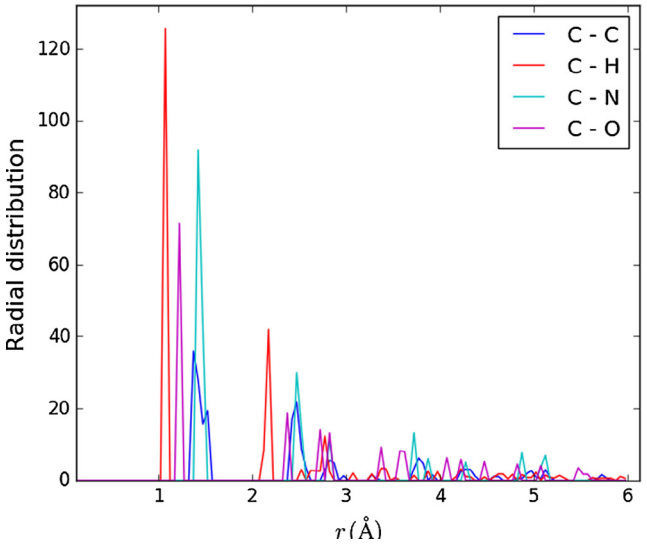

Fig. 11. The radial distribution functions (RDFs) of the carbon-carbon (C-C), carbon-hydrogen (C-H), carbon-nitrogen (C-N) and carbon-oxygen (C-O) interactions of PTCDI-C5 in chloroform solvent.

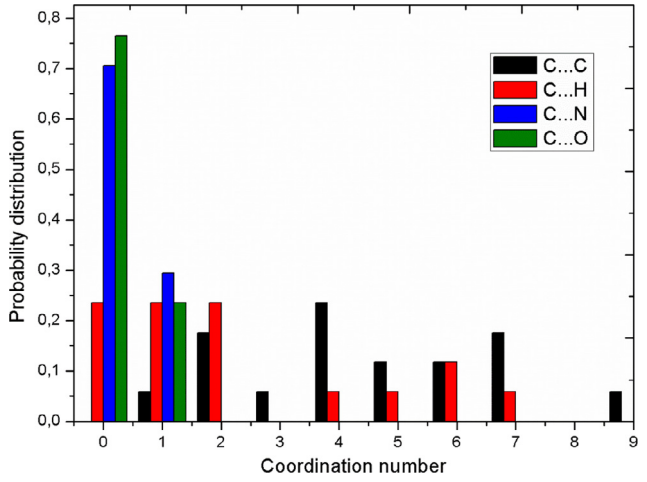

Fig. 12. Probability distributions of the carbon-carbon (C-C), carbon-hydrogen (C-H), carbon-nitrogen (C-N) and carbon-oxygen (C-O) interactions of PTCDI-C5 depending on coordination number in chloroform solution.

5. Conclusions

PTCDI-C5 organic nanostructure have been investigated via experimental and theoretical techniques. The results showed that the structure with minimum total energy of the PTCDI-C5 is the C_1 form. Experimental molar extinction coefficients exhibit three dominant peaks visible region. The maximum peak is found to be compatible with theoretical value for chloroform and toluene solvents. The direct refractive index values are lower than the indirect ones. The increase in the concentrations causes an increase in the direct and indirect refractive index values. The electrical conductance can be controlled with concentrations thus it provides an advantage for electronic and optoelectronic devices. The increase in thickness of PTCDI-C5 samples gives rise to the dispersion of the electronic bands thus decrease the band gap energies. Predicted band energy values for different solvents are also agreement with the experimental data. In addition, C-H interactions has a narrower and higher distribution.

Acknowledgments

The numerical calculations reported in this paper were partially performed at TUBITAK ULAKBIM, High Performance and Grid Computing Centre (TRUBA resources). This study was supported by The Management Unit of Scientific Research Projects of Muş Alparslan University (MUSBAP) under Project 0001.

References

[1] A.A.M. Farag, B. Gunduz, F. Yakuphanoglu, W.A. Farooq, Synth. Met. 160 (2010) 2559.
[2] T. Hori, T. Masuda, N. Fukuoka, T. Hayashi, Y. Miyake, T. Kamikado, H. Yoshida, A. Fujii, Y. Shimizu, M. Ozaki, Org. Electron. 13 (2012) 335.
[3] S. Rajaram, R. Shivanna, S.K. Kandappa, K.S. Narayan, J. Phys. Chem. Lett. 3 (2012) 2405.
[4] B. Gunduz, I.S. Yahia, F. Yakuphanoglu, Microelectron. Eng. 98 (2012) 41.
[5] M.Y. Ameen, T. Abhijith, D. Susmita, S.K. Ray, V.S. Reddy, Org. Electron. 14 (2013) 554.
[6] M. Neghabia, A. Behjata, Curr. Appl. Phys. 12 (2012) 597.
[7] F. Aziz, M.H. Sayyad, K. Sulaiman, B.Y. Mailis, K.S. Karimov, Z. Ahmad, G. Sugandi, Meas. Sci. Technol. 23 (2012) 014001.
[8] M. Murugavelu, P.K.M. Imran, K.R. Sankaran, S. Nagarajan, Mater. Sci. Semicon. Proc. 16 (2013) 461.
[9] G. Harsaanyi, Sens. Rev. 20 (2000) 98.
[10] Y. Che, X. Yang, G. Liu, C. Yu, H. Ji, J. Zuo, J. Zhao, L. Zang, J. Am. Chem. Soc. 132 (2010) 5743.
[11] Y. Huang, R. Yuan, S. Zhou, J. Mater. Chem. 22 (2012) 883.
[12] Y. Huang, L. Fu, W. Zou, F. Zhang, New J. Chem. 36 (2012) 1080.
[13] J.B. Wang, W.L. Li, B. Chu, C.S. Lee, Z.S. Su, G. Zhang, S.H. Wu, F. Yan, Org. Elec. 12 (2011) 34.
[14] X. Zeng, T. Zhou, C. Leng, Z. Zang, M. Wang, W. Hu, X. Tang, S. Lu, L. Fang, M. Zhou, J. Mater. Chem. A 5 (2017) 17499.
[15] H. Ma, N. Liu, J.-D. Huang, Sci. Rep. 7 (1) (2017), art. no. 331.
[16] C. Sutton, J.S. Sears, V. Coropceanu, J.-L. Brédas, J. Phys. Chem. Lett. 4 (6) (2013) 919.
[17] F. Würthner, Chem. Commun. 14 (2004) 1564.
[18] B. Gündüz, Opt. Mater. 36 (2013) 425.
[19] C.C. Chao, M.K. Leung, J. Org. Chem. 70 (2005) 4323.
[20] L. Fan, Y. Xu, H. Tian, Tetrahedron Lett. 46 (2005) 4443.
[21] H. Dinçalp, Ş. Kızılok, S. İçli, Dyes Pigments 86 (2010) 32.
[22] R.T. Weitz, K. Amsharov, U. Zschieschang, E.B. Villas, D.K. Goswami, M. Burghard, H. Dosch, M. Jansen, K. Kern, H. Klauk, J. Am. Chem. Soc. 130 (2008) 4637.
[23] Z. Yuan, J. Li, Y. Xiao, Z. Li, X. Qian, J. Org. Chem. 75 (2010) 3007.
[24] G. Boobalan, P. Mohamed Imran, S. Nagarajan, Chin. Chem. Lett. 23 (2012) 149.
[25] C.W. Struijk, A.B. Sievel, J.E.J. Dakhorst, M.V. Dijk, P. Kimkes, R.B.M. Koehorst, H. Donker, T.J. Schaafsma, S.J. Picken, A.M.W. Craats, J.M. Warman, H. Zuilhof, E.J. R. Sudholter, J. Am. Chem. Soc. 122 (45) (2000) 11057.
[26] E.W. Meijer, A. Schenning, P. H. J, Nature 419 (2002) 353.
[27] R.J. Chesterfield, J.C. McKeen, C.R. Newman, P.C. Ewbank, D.A. da Silva Filho, J.-L. Bredas, L.L. Miller, K.R. Mann, C. Frisbie, D, J. Phys. Chem. B 108 (2004) 19281.
[28] K. Balakrishnan, A. Datar, R. Oitker, H. Chen, J. Zuo, L. Zang, J. Am. Chem. Soc. 127 (2005) 10496.
[29] P.K. Sekhar, E.L. Brosha, R. Mukundan, K.L. Linker, C. Brusseau, F.H. Garzon, J. Hazard Mater. 190 (2011) 125.
[30] Y. Huang, J. Wang, L. Fu, W. Kuang, J. Shi, Sens. Actuators, B 188 (2013) 411.
[31] H. Peng, L. Ding, T. Liu, X. Chen, L. Li, S. Yin, Y. Fang, Chem. – Asian J. 7 (2012) 1576.
[32] Alejandro L. Briseno, Stefan C.B. Mannsfeld, Colin Reese, Jessica M. Hancock, Yujie Xiong, Samson A. Jenekhe, Zhenan Bao, Younan Xia, Younan Xia, Nano Lett. 7 (2007) 2847.
[33] Bayram Gündüz, Sensor Lett. 13 (1) (2015) 52.
[34] Bayram Gündüz, Polym. Adv. Technol 27 (2) (2015) 144.
[35] W. Kohn, L.J. Sham, Phys. Rev. 140 (1965) A1133.
[36] A.D. Becke, Phys. Rev. A 38 (1988) 3098.
[37] S.H. Vosko, L. Vilk, M. Nusair, Can. J. Phys. 58 (1980) 1200.
[38] C. Lee, W. Yang, R.G. Parr, Phys. Rev. B 37 (1988) 785.
[39] M.J. Frisch, G.W. Trucks, H.B. Schlegel, G.E. Scuseria, M.A. Robb, J.R. Cheeseman, G. Scalmani, V. Barone, B. Mennucci, G.A. Petersson, et al., Gaussian 09, Revision B.01, Gaussian, Inc., Wallingford CT, 2009.
[40] A. Beer, Ann. Phys. 86 (1852) 78.
[41] S.K. Tripathy, Opt. Mater. 46 (2015) 240.
[42] M. Cabuk, B. Gündüz, Appl. Surf. Sci. 424 (2017) 345.
[43] J.O. Akinlami, I.O. Olateju, Semicond. Phys Quantum Electron. 153 (2012) 281.
[44] C.R. Newman, C.D. Frisbie, et al., Chem. Mater. 16 (2004) 4436.
[45] M.C.R. Delgado, E.-G. Kim, et al., J. Am. Chem. Soc. 132 (2010) 3375.
[46] E. Erdoğan, B. Gündüz, Electron. Mater. Lett. 12 (2016) 773.
[47] M. Kurban, Ş. Erkoç, J. Comput. Theor. Nanosci. 12 (2015) 2605.
[48] M. Kurban, B. Gündüz, J. Mol. Struct. 1137 (2017) 403.
[49] N.M. O'Boyle, A.L. Tenderholt, K.M. Langer, J. Comput. Chem. 29 (2008) 839.